DOI: 10.1002/ejic.200500730

Synthesis and X-ray Crystal Structures of the New, Three-Dimensional Ethylenediphosphonates $[A\{HO_3P(CH_2)_2PO_3H_2\}]$ (A = Alkali Metal, Tl, or NH_4): Solid Brönsted Acids That Exhibit Topotactic Intercalation and Deintercalation of Ammonia

Koya Prabhakara Rao[a] **and Kanamaluru Vidyasagar***[a]

Keywords: Intercalation / Organic–inorganic hybrid composites / Phosphonates / X-ray diffraction

Seven new ethylenediphosphonates with the formula $[A\{HO_3P(CH_2)_2PO_3H_2\}]$ [A = Li (**1**), Na (**2**), K (**3**), Rb (**4**), Cs (**5**), Tl (**6**), and NH_4 (**7**)], have been synthesized and characterized by single-crystal X-ray diffraction, infrared spectroscopy, and thermal studies. They have four types of three-dimensional structures, with variations in the coordination of the A^+ ions. All of them are solid Brönsted acids that undergo room-temperature, acid–base intercalation reactions with ammonia.

Introduction

Metal organophosphonates are a class of organic–inorganic hybrid materials in which the organophosphonate groups are covalently bonded to the metal inorganic backbone. In the recent past, there has been a renewed interest and activity in the research area of metal organophosphonates,[1–6] mainly due to their varied compositions, structural diversity, and potential applications,[7–11] for example, as sorbents, ion-exchangers, sensors, and catalysts. The expansion of metal organophosphonate chemistry includes phosphonates[12–15] and diphosphonates[16–18] of s-, p-, d- and f-block metals, and the structures reported for these compounds can be broadly classified into two categories, namely zero-dimensional types, such as mononuclear and complex molecular clusters, and extended framework types like one-, two-, and open three-dimensional networks. Low-dimensional structures such as chains and layers are mostly observed for compounds of the second type due to the segregation of hydrophobic regions of the organic moieties from the rest of the framework.

The solid-state chemistry of diphosphonates[16–18] is an emerging area of research, and several investigations concerning the synthesis, structures, and properties of di-, tri-, and tetravalent metal diphosphonates with extended frameworks,[16–18] such as $(VO)_2[CH_2(PO_3)_2]{\cdot}4H_2O$, $[Ti_3O_2(H_2O)_2(O_3PCH_2PO_3)_2]{\cdot}(H_2O)_2$, $[Al_2\{(O_3PCH_2CH_2PO_3)\}(H_2O)_2F_2]{\cdot}H_2O$, $[Al_2\{(O_3PC_2H_4PO_3)_{1-x}(HPO_3)_{2x}\}(H_2O)_2F_2]{\cdot}H_2O$ ($0 \le x \le 0.32$), $[Al_2(OH)_2(H_2O)_2(O_3PCH_2CH_2PO_3)]$, $[Ga_2\{(O_3PCH_2CH_2PO_3)\}(H_2O)_2F_2]{\cdot}2H_2O$, $[Sb_2\{O(O_3PCH_2PO_3H)\}]$, $[Ni_4(O_3PCH_2PO_3)_2]{\cdot}(H_2O)_n$ (n = 3, 2, 0), $[Cr_2\{O_3P\text{-}(CH_2)_2\text{-}PO_3\}_2]{\cdot}3H_2O$, $[Cu_2\{(O_3PCH_2CH_2PO_3)(H_2O)_2\}]$, $[Cu_2\{(O_3PC_3H_6PO_3)(H_2O)_2\}]{\cdot}H_2O$, $[Cu_2\{(O_3PC_4H_8PO_3)(H_2O)_2\}]{\cdot}2H_2O$, $[Cu_2\{(O_3PC_5H_{10}PO_3)(H_2O)_2\}]{\cdot}2.8H_2O$, $[Zn_2\{(O_3PCH_2CH_2PO_3)_2(H_2O)\}]$, $[Zn_2\{(O_3PC_3H_6PO_3)\}]$, $[Co_2(O_3PCH_2PO_3)]{\cdot}H_2O$, $[Fe_2\{(O_3PCH_2CH_2PO_3)\}]$, and $[Fe_2\{(O_3PCH_2CH_2PO_3)\}]{\cdot}2H_2O$, have been reported. These examples illustrate the structural diversity and the compositional variations, with different ratios of metal to diphosphonates, inclusion of F^-, O^{2-}, and/or H_2O in the coordination sphere of the metals, and di-, tri-, and tetraanionic forms of diphosphonic acids with different alkyl chain lengths. One noteworthy feature of all these alkyl diphosphonates is their insolubility in water, which enables their isolation as precipitates from aqueous solutions.

Among the many diphosphonates reported, there are only a few reports[18] of compounds with a metal to diphosphonic acid ratio of 1:1. These include $[Ti\{O_3P(CH_2)_nPO_3\}]$ (n = 2, 3), $[LnH\{O_3P(CH_2)_nPO_3\}]$ (n = 1–3), $[Sb\{O_3P(CH_2)_nPO_3H\}]$ (n = 2, 3), and $[Sn(HO_3PCH_2PO_3H)]$. These tri- and divalent metal compounds contain $(HO_3PCH_2PO_3H)^{2-}$ and $(HO_3PCH_2PO_3)^{3-}$ anions and are, therefore, potential solid Brönsted acids. However, there are no reports of the intercalation properties of these diphosphonates. It is in this context that 1:1 diphosphonates of monovalent metals, $[A\{HO_3P(CH_2)_nPO_3H_2\}]$, are envisaged to be strong, solid Brönsted acids that can undergo intercalation with bases. Only two monovalent metal diphosphonates, namely $[Ag_4\{O_3P(CH_2)_2PO_3\}]$ and $[Na\{HO_3PCH_2PO_3H_2\}]$, have been reported[19] so far. We have recently synthe-

---

[a] Department of Chemistry,
Indian Institute of Technology Madras,
Chennai, 600036, India
E-mail: kvsagar@iitm.ac.in

Supporting information for this article is available on the WWW under http://www.eurjic.org or from the author.

sized[20] seven new, low-dimensional 1:2 phenylphosphonates of monovalent metals, [A(HO_3PPh)(H_2O_3PPh)] (A = Li, Na, K, Rb, Cs, NH_4, and Tl). These solid Brönsted acids undergo intercalation of amines and ammonia and, in a few cases, to the largest extent ever known. In view of these observations, we have undertaken a study of 1:1 metal alkyl diphosphonates of alkali and thallium metals and ammonium. We report here the successful synthesis, characterization, and ammonia-intercalation of the new, water-soluble ethylene diphosphonates [A{$HO_3P(CH_2)_2PO_3H_2$}] [A = Li (**1**), Na (**2**), K (**3**), Rb (**4**), Cs (**5**), Tl (**6**), and NH_4 (**7**)].

Results and Discussion

X-ray Diffraction and Crystal Structures

The observed powder XRD patterns for all the seven structurally characterized [A{$HO_3P(CH_2)_2PO_3H_2$}] compounds agree with those simulated with the LAZY-PULVERIX program[21] on the basis of single-crystal X-ray structures, thus indicating the single-phase nature of the samples. However, the observed relative intensities of some of the reflections are different from those calculated due to the preferential orientation of the crystallites. The crystal structures of ethylenediphosphonates **1**–**7** can be broadly classified into four structural types, namely those of compounds **1**, **2**, **3**, and **7**. From the point of view of A-P-O frameworks the sodium compound is two-dimensional, whereas the others are all one-dimensional compounds. However, these frameworks are connected three-dimensionally by the ethylene moiety.

[Li{$HO_3P(CH_2)_2PO_3H_2$}] (**1**) contains half of one unit formula in the asymmetric unit. The lithium atom sits on a twofold axis and is tetrahedrally bonded to four O(1) atoms, which are near the inversion center 4b. Each $LiO(1)_4$ tetrahedron shares two edges with two such tetrahedra to form "LiO_2" chains parallel to the *c*-axis (Figure 1). O(1) is bonded to two Li atoms, and each diphosphonate, in turn, is bonded to four Li atoms, linking two such "LiO_2"chains. The ethylenediphosphonate groups connect these chains three-dimensionally. The four phosphonate moieties of different diphosphonates are positioned near the inversion center 4a such that O(3)–H(3) forms a hydrogen bond with O(2) and the other acidic hydrogen atom, H(2), at the inversion center is between two O(2) atoms, as shown in the encircled region of Figure 1. This unique region of space could be conceived as being porous. To the best of our knowledge this is the first lithium diphosphonate.

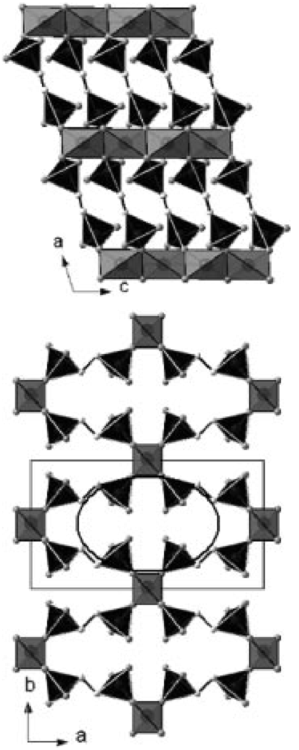

Figure 1. Polyhedral representation of the unit cell of [Li{$HO_3P(CH_2)_2PO_3H_2$}] (**1**) viewed along the *b*-axis (top) and the *c*-axis (bottom).

[Na{$HO_3P(CH_2)_2PO_3H_2$}] (**2**) contains two formula units in the asymmetric unit. The two crystallographically distinct sodium atoms, Na1 and Na2, are confined approximately to the *xy* planes at $z \approx 1/4$ and $3/4$ and octahedrally coordinated to ten of twelve crystallographically distinct oxygen atoms [O(1)–O(12)]. Only O(8) and O(11) are not bonded to sodium atoms. These two NaO_6 octahedra share the O(7)–O(10) edge to form a Na_2O_{10} unit, which is linked to ten phosphonate moieties of five diphosphonates (Figure 2). Thus, the diphosphonates connect Na_2O_{10} units in the same plane as well as those in the adjacent planes, leading to a layered–pillared structure (Figure 2). The two diphosphonates are distinct in that one is bonded to six sodium atoms whereas the other is bonded to only four.

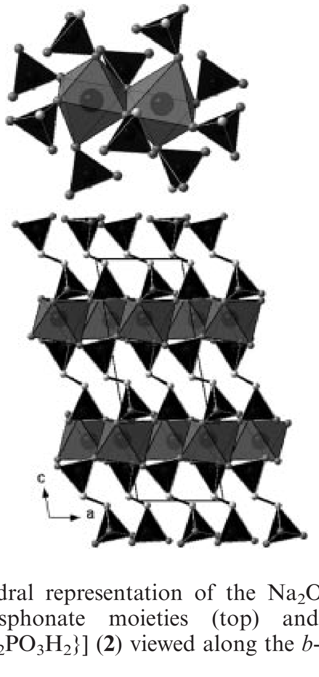

Figure 2. Polyhedral representation of the Na_2O_{10} bi-octahedral unit with phosphonate moieties (top) and unit cell of [Na{$HO_3P(CH_2)_2PO_3H_2$}] (**2**) viewed along the *b*-axis (bottom).

[K{$HO_3P(CH_2)_2PO_3H_2$}] (**3**) has one formula unit in the asymmetric unit. The potassium atoms are confined approximately to the *xz* planes at $y \approx 1/4$ and $3/4$ and coordinated dodecahedrally to oxygen atoms O(1)–O(6) of the diphosphonate, with the maximum value of the K–O bond length being 3.073(2) Å. Each KO_8 dodecahedron shares two O(1)–O(4) edges with two such polyhedra to form "KO_6" chains parallel to the *c*-axis (Figure 3). These chains are linked to one another three-dimensionally by diphosphonate moieties through the O(5) atoms. Thus, this compound is three-dimensional in nature. The diphosphonate is coordinated to five potassium atoms. Similarly, each potassium atom is bonded to five phosphonate moieties of different diphosphonates: three of them are bonded in a bidentate fashion and other two in a monodentate fashion. O(3)–H(3) and O(6)–H(6) form hydrogen bonds with O(1) and O(4), respectively. H(2) and H(5), at two inversion centers, represent two disordered positions of the other acidic hydrogen atom and are located, respectively, between the O(2) and O(5) atoms. These structural features are present in the similar three-dimensional rubidium (**4**), cesium (**5**), and thallium (**6**) compounds as well.

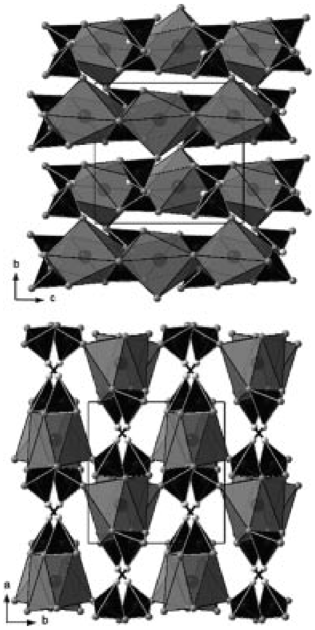

Figure 3. Polyhedral representation of the unit cell of [$K\{HO_3P(CH_2)_2PO_3H_2\}$] (**3**) viewed along the *a*-axis (top) and the *c*-axis (bottom).

The rubidium (**4**) and cesium (**5**) compounds have the same positional parameters and contain half a formula unit in their asymmetric units. The metal atoms sit on twofold axes and are dodecahedrally coordinated to the O(1)–O(3) atoms of a diphosphonate moiety. The maximum values of the Rb–O and Cs–O bond lengths are 3.199(3) and 3.431(3) Å, respectively. Each AO_8 dodecahedron shares two O(1)–O(1)′ edges with two such polyhedra to form "AO_6" chains parallel to [101]. These chains are linked to one another three-dimensionally, by diphosphonate moieties, through the O(1) atoms. Unlike cesium, which is bonded to eight diphosphonates in a monodentate fashion, rubidium is bonded to two diphosphonates in a bidentate fashion and another four in a monodentate mode. The hydrogen bonding is the same in both compounds: O(3)–H(3) forms a hydrogen bond with O(2) and the other acidic hydrogen atom, H(2), at the inversion center is between two O(2) atoms.

There are two distinct diphosphonates, which sit on inversion centers 2b and 2d, in the unit cell of [$Tl\{HO_3P(CH_2)_2PO_3H_2\}$] (**6**). The thallium atoms are confined approximately to the *yz* planes at $x \approx 0.27$ and 0.77 and are coordinated dodecahedrally to oxygen atoms O(1)–O(6) of both diphosphonates, with the maximum value of the Tl–O bond length being as high as 3.47(3) Å. TlO_8 dodecahedra, similar to those in the potassium compound, share O(1)–O(1) and O(6)–O(6) edges to form "TlO_6" chains parallel to the *a*-axis; these chains are linked to one another through the O(4) atoms. The diphosphonate is bonded, in a monodentate fashion, to six thallium atoms. Similarly, the thallium atom is bonded to six phosphonate moieties of different diphosphonates. Both O(3)–H(3) and O(6)–H(6) form hydrogen bonds with O(5). H(2) and H(5), with half site-occupancies, represent two disordered positions of the other acidic hydrogen atom and are bonded, respectively, to the O(2) and O(5) atoms. O(2)–H(2) and O(5)–H(5) form hydrogen bonds with O(4) and O(3), respectively.

The nitrogen atoms in [$NH_4\{HO_3P(CH_2)_2PO_3H_2\}$] (**7**) are confined approximately to the *ab* planes and are tetrahedrally hydrogen-bonded to oxygen atoms of the diphosphonates (Figure 4). The two crystallographically distinct ethylene diphosphonates sit on inversion centers 1h and 1b. All the six oxygen atoms, represented by O(4)–O(6), of one diphosphonate and only two oxygen atoms, O(1) and O(1)′, of another diphosphonate are hydrogen-bonded to nitrogen. The connectivity pattern of NO_4 tetrahedra and "PO_3C" phosphonate moieties results in ladder-like chains parallel to the *a*-axis (Figure 4), with porous regions between them. Such a pattern is also observed[20] in [$NH_4(HO_3PC_6H_5)(H_2O_3PC_6H_5)$]. These chains in the adja-

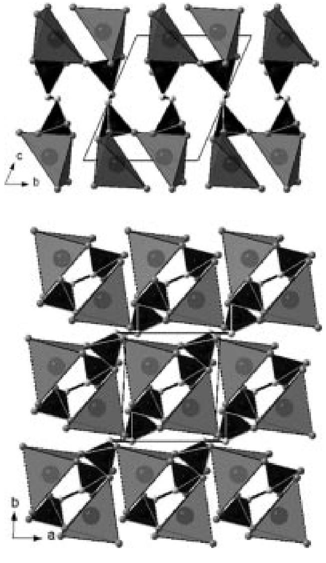

Figure 4. Polyhedral representation of the unit cell of [$NH_4\{HO_3P(CH_2)_2PO_3H_2\}$] (**7**) viewed along the *a*-axis (top) and the *c*-axis (bottom).

cent layers are connected three-dimensionally through the C–C bonds of the PO_3C phosphonate moieties. O(3)–H(3) and O(6)–H(6) form hydrogen bonds with O(4) and O(1), respectively, and O(2)–H(2) is strongly hydrogen bonded to O(5).

In the five compounds **1**, **3**, **4**, **5**, and **7**, the values of the P–O, P–C, and C–C bond lengths vary in the ranges 1.493(3)–1.575(2), 1.790(4)–1.795(3), and 1.522(5)–1.542(7) Å, respectively. These values compare with the 1.501(1)–1.553(2) Å range of P–O bond lengths, the 1.786(2) Å P–C bond length, and the 1.544(4) Å C–C bond length reported[22] for ethylenediphosphonic acid. The corresponding bond-length ranges of 1.48(2)–1.590(7), 1.74(3)–1.89(1), and 1.45(2)–1.55(2) Å in compounds **2** and **6** are a bit wider.

Spectroscopic Studies

All seven compounds, as illustrated for **1** in Figure 5, have the following common infrared spectral features: (i) the C–H stretching vibrations[17c] of the ethylenediphosphonate group are observed around 2970 and 2924 cm^{-1}, whereas their bending vibrations are seen at 1380 cm^{-1}; (ii) the peaks in the region 1200–1000 cm^{-1} are due to P–O stretching vibrations and the O–P–O bending vibrations[17c] are found in the region 540–410 cm^{-1}. The infrared spectrum of the ammonium compound shows two additional peaks at 3240 and 1401 cm^{-1} corresponding to the stretching and bending vibrations of the ammonium ion.[23]

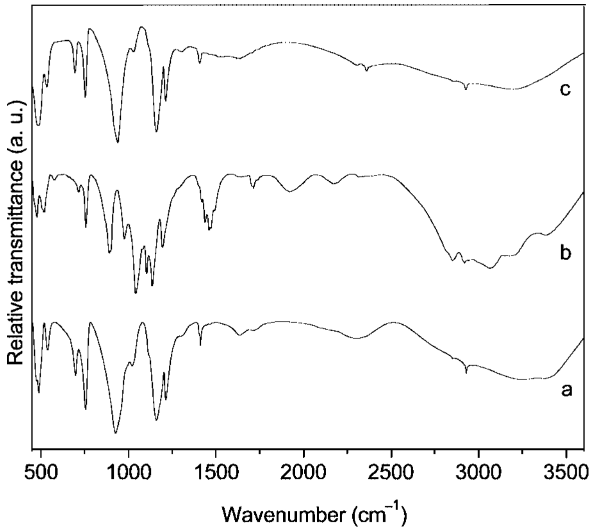

Figure 5. Infrared spectra of $[Li\{HO_3P(CH_2)_2PO_3H_2\}]$ (**1**) (a), its intercalate **1**·$(NH_3)_{1.5}$ (b) and deintercalate (c).

Thermal Analysis

Thermogravimetric analysis of all the seven compounds was carried out. The thermogravimetric curves of compounds **1**, **2**, and **7** are presented in Figure 6. No efforts have been made to identify the composition of the intermediate, residual solid products of decomposition and, therefore, only a factual description of these thermogravimetric curves is given. All these compounds are stable up to about 170–200 °C. Compounds **1**–**6** undergo total weight losses of 22.5–30% in the temperature range 200–800 °C, whereas the ammonium compound **7** has a maximum weight loss of 75%. These weight losses occur in two steps, with the second one at 460 °C being the major one.

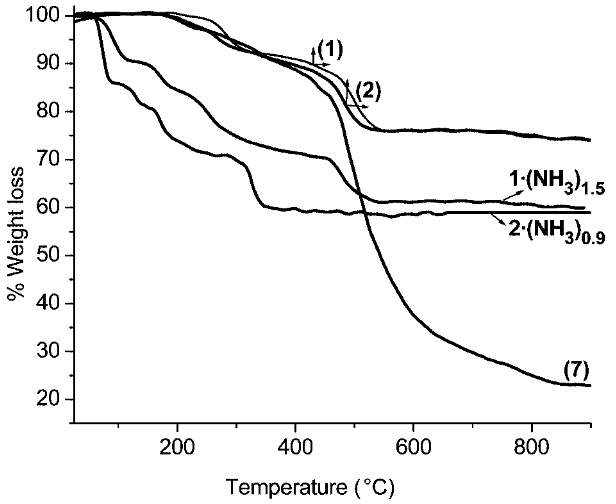

Figure 6. Thermogravimetric curves of compounds $[A\{HO_3P(CH_2)_2PO_3H_2\}]$ [A = Li (**1**), Na (**2**), and NH_4 (**7**)] and ammonia intercalates **1**·$(NH_3)_{1.5}$ and **2**·$(NH_3)_{0.9}$.

Intercalation and Deintercalation Reactions

All these ethylenediphosphonates are solid Brönsted acids. For example, the pH values of 1 M solutions of pure ligand and the sodium compound **2** are 2 and 3, respectively. Therefore, they were examined from the point of view of acid–base intercalation reactions with ammonia. These reactions, as determined from chemical analysis and spectroscopic and thermal studies, turned out to be successful. The success and extent of ammonia intercalation in the intercalates (**1**–**7**)·$(NH_3)_x$ were determined from the IR spectra and elemental analysis. The IR spectra (Figure 5) of compounds, (**1**–**6**)·$(NH_3)_x$ contain two additional peaks at 3240 and 1450 cm^{-1} corresponding to the stretching and bending vibrations of the ammonium ion.[24] The x values of (**1**–**7**)·$(NH_3)_x$ are 1.5, 0.9, 0.7, 0.5, 0.4, 1.0, and 1.6 respectively, and indicate partial intercalation and no systematic variation with the size and nature of A. The large value of x for the lithium and ammonium compounds corroborates their large porosity and greater access to the porous regions. The differences in the powder XRD patterns of the parent diphosphonate and its ammonium intercalate are significant in the case of **1**, **3**, **6**, and **7**, which is indicative of intercalation of ammonia into the porous regions of the structure. However, the overall crystallinity decreases, as shown for **1**·$(NH_3)_{1.5}$ in Figure 7. Unlike the parent phases, the intercalates undergo a greater percentage of weight loss and begin to decompose at lower temperatures. This is illustrated by the thermogravimetric curves of **1**·$(NH_3)_{1.5}$ and **2**·$(NH_3)_{0.9}$ in Figure 6. We also carried out ammonia deintercalation for a few selected intercalates, namely those of **1**, **2**, and **7**. They undergo deintercalation upon heating in the air-oven at about 170 °C for about 12 hours. The IR spectra (Figure 6), elemental analysis, and powder XRD patterns (Figure 7) of the deintercalated products, as illustrated in the case of **1**·$(NH_3)_{1.5}$, confirm that the deintercalation is complete and topotactic. To the best of our knowledge, this is the first time that such a reversible intercalation of ammonia in hybrid materials has been demonstrated.

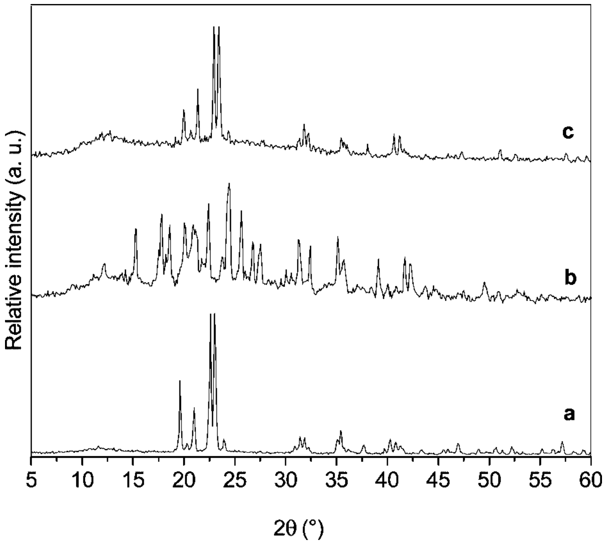

Figure 7. Powder X-ray diffraction patterns of $[Li\{HO_3P(CH_2)_2PO_3H_2\}]$ (**1**) (a), its intercalate **1**·$(NH_3)_{1.5}$ (b) and deintercalate (c).

$[Zn(O_3PPh)]$ and $[UO_2(HO_3PPh)_2(H_2O)]_2 \cdot 8H_2O$ have been reported[9,25] to be sensors and proton conductors due to their intercalation and Brönsted-acidic properties, respectively. Compounds **1**–**7** exhibit both these properties and could be potentially useful as sensors and proton conductors.

Concluding Remarks

A series of seven, new ethylenediphosphonates, $[A\{HO_3P(CH_2)_2PO_3H_2\}]$ (A = alkali metal, Tl and NH_4), have four types of three-dimensional porous structures. They are solid Brönsted acids and undergo room-temperature intercalation reactions with ammonia. These intercalates can be deintercalated topotactically.

Experimental Section

Synthesis: The high purity chemicals A_2CO_3 [A = Li, Na, K, NH_4 (SD Fine, India), Rb, Cs and Tl (Aldrich)] and 1,2-ethylenediphosphonic acid ($H_2O_3PCH_2CH_2PO_3H_2$, Lancaster) were used as purchased. The compounds $[A\{HO_3P(CH_2)_2PO_3H_2\}]$ [A = Li (**1**), Na (**2**), K (**3**), Rb (**4**), Cs (**5**), Tl (**6**), and NH_4 (**7**)] were synthesized, on a 0.5–1.0-g scale, by evaporating aqueous solutions of stoichiometric reactant mixtures of ethylenediphosphonic acid and the appropriate carbonate. Slow evaporation, at room temperature, led to the formation of compounds as colorless, block-shaped or flaky crystals. However, evaporation in a steam bath yielded products in a polycrystalline form. In all the cases the yields were almost quantitative. These seven compounds were ascertained to be pure by elemental analysis with a Perkin–Elmer series 11 Model analyzer. $C_2H_7LiO_6P_2$ (195.96): calcd. C 12.25, H 3.60; found C 12.42, H 3.67. $C_2H_7NaO_6P_2$ (212.01): calcd. C 11.33, H 3.33; found C 11.80, H 3.38. $C_2H_7KO_6P_2$ (228.12): calcd. C 10.53, H 3.09; found C 10.61, H 3.00. $C_2H_7O_6P_2Rb$ (274.49): calcd. C 8.75, H 2.57; found C 8.62, H 2.67. $C_2H_7CsO_6P_2$ (321.93): calcd. C 7.46, H 2.19; found C 7.68, H, 2.23. $C_2H_7O_6P_2Tl$ (393.39): calcd. C 6.11, H 1.79; found C 6.15, H 1.79. $C_2H_{11}NO_6P_2$ (207.06): calcd. C 11.60, H 5.35, N 6.76; found C 11.62, H 5.22, N 6.50.

Ammonia Intercalation and Deintercalation Reactions: Intercalation of ammonia was achieved by passing ammonia gas over solid samples of ethylenediphosphonates **1**–**7** for 2 h. The amount (*x*) of intercalated ammonia was determined by analysis of the CHN content of the solid intercalates (**1**–**7**)·$(NH_3)_x$. Ammonia deintercalation was carried out by heating a sample of the intercalate in an oven at 170 °C for 12 h.

X-ray Diffraction and Crystal Structure: The powder X-ray diffraction (XRD) patterns of the seven ethylenediphosphontes **1**–**7** and their ammonia-intercalation products were recorded on a Shimadzu XD-D1 X-ray diffractometer using Cu-K_α (λ = 1.5406 Å) radiation. Single crystals of compounds **1**–**7** suitable for X-ray diffraction were selected and mounted with glue on thin glass fibers. Crystals of compound **7** were found to be twinned. The X-ray data were gathered successfully at 25 °C, on an ENRAF-NONIUS CAD4 automated four-circle diffractometer, by standard procedures involving ω–2θ techniques. These data sets were reduced by routine computational procedures. The program SHELXL-97[26] (Wingx) was employed for the structure solution and refinements and the graphic program DIAMOND[27] was used to draw the structures. The structure solutions were obtained by Patterson's method for compound **6** and by direct methods for the others. O(10) of **2** and O(1) of **6** were refined isotropically, whereas all other non-hydrogen atoms of these seven compounds were refined anisotropically. In each phosphonate moiety of compounds **1**–**7** the three oxygen atoms were labeled in increasing order of P–O bond lengths as they are different from one another. The oxygen atoms with short P–O bonds were considered to be formally double bonded to phosphorus atoms. The non-hydrogen-atom contents do not account for charge neutrality, thus indicating the presence of three acidic protons of diphosphonic acid moieties. These acidic hydrogen atoms, for all compounds except **2**, were located in the difference Fourier maps and refined with riding model restraints. Two of the three acidic hydrogen atoms of diphosphonate are bonded to the two oxygen atoms with long P–O bonds, whereas the third hydrogen atom is bonded to, or located between, those oxygen atoms with intermediate P–O bond lengths.[28] The ethylene hydrogen atoms were refined for all the seven compounds. For the ammonium compound **7**, the ammonium hydrogen atoms were located in the difference Fourier map and included in the final refinement. The structure refinement proceeded smoothly for all compounds but **2** and **6**. For compound **2**, the *R* value was 10.5% and therefore an additional absorption correction, based on the isotropically refined model, was applied to the X-ray data using the program DIFABS.[29] The final difference Fourier map showed no residual peak with electron density of $>1\,e\text{Å}^{-3}$ and the final *R* value improved to around 7.8%. The C(2)–C(2)′ and C(4)–C(4)′ bond lengths in **2** were constrained to be 1.55 Å. For the thallium

Table 1. Pertinent crystallographic data for [AH{$HO_3P(CH_2)_2PO_3H$}] [A = Li (**1**), Na (**2**), K (**3**), Rb (**4**), Cs (**5**), Tl (**6**), and NH_4 (**7**)].

Compound	**1**	**2**	**3**	**4**	**5**	**6**	**7**
Formula	$LiP_2O_6C_2H_7$	$NaP_2O_6C_2H_7$	$KP_2O_6C_2H_7$	$RbP_2O_6C_2H_7$	$CsP_2O_6C_2H_7$	$TlP_2O_6C_2H_7$	$NP_2O_6C_2H_{11}$
Formula weight	195.96	212.01	228.12	274.49	321.93	393.39	207.06
Crystal system	monoclinic	triclinic	monoclinic	monoclinic	monoclinic	monoclinic	triclinic
a [Å]	16.188(2)	5.727(8)	9.237(1)	10.980(3)	11.472(7)	8.589(3)	6.176(1)
b [Å]	8.503(2)	7.957(4)	8.909(2)	9.490(4)	11.030(4)	8.930(4)	7.723(3)
c [Å]	5.381(2)	16.52(2)	9.484(2)	9.222(2)	8.443(3)	10.094(3)	9.183(2)
α [°]	90	101.5(1)	90	90	90	90	66.70(2)
β [°]	107.92(1)	97.82(9)	92.60(2)	120.91(2)	127.90(4)	90.05(5)	85.78(2)
γ [°]	90	98.8(1)	90	90	90	90	85.57(3)
V [Å^3]	704.7(3)	718.4(12)	779.6(3)	824.5(4)	843.0(6)	774.2(5)	400.6(2)
Space group	$C2/c$ (no. 15)	$P\bar{1}$ (no. 2)	$P2_1/c$ (no. 14)	$C2/c$ (no. 15)	$C2/c$ (no. 15)	$P2_1/c$ (no. 14)	$P\bar{1}$ (no. 2)
Z	4	4	4	4	4	4	2
$\rho_{\text{calcd.}}$ [g cm^{-3}]	1.847	1.960	1.944	2.211	2.537	3.375	1.716
μ(Mo-K_α) [mm^{-1}]	0.593	0.645	1.074	6.376	4.756	21.256	0.531
Total reflections	631	2799	1455	765	783	2880	1436
Independent reflections	614	2523	1372	724	745	1348	1415
$R^{[a]}$	0.0309	0.0775	0.0241	0.0237	0.0253	0.0800	0.0291
$R_w^{[b]}$	0.0864	0.2373	0.0699	0.0663	0.0677	0.1882	0.0814

[a] $R = \Sigma||F_o| - |F_c||/\Sigma|F_o|$. [b] $R_w = [\Sigma w(|F_o|^2 - |F_c|^2)^2/\Sigma w(|F_o|^2)^2]^{1/2}$.

compound **6**, refinement with correction for twin crystal-data was carried out. The final R value was about 8% and the final difference Fourier map showed twenty ghost residual peaks with electron density greater than 1 e Å^{-3}. No additional absorption correction was applied to the X-ray data, as it could not improve the R value. The R_w values for **2** and **6** are a bit high and the desired improvisation of crystal structure refinement, for lower values, was not possible. However, the qualitative picture of these structures is totally correct and the quantitative details are, to a large extent, also correct. The pertinent crystallographic data of all these seven ethylenediphosphonates are presented in Table 1.

CCDC-281082, -281083, -281084, -281085, -281086, -281087 and -281088 (for **1**–**7**) contain the supplementary crystallographic data for this paper. These data can be obtained free of charge from The Cambridge Crystallographic Data Centre via www.ccdc.cam.ac.uk/data_request/cif.

Infrared Spectroscopic and Thermogravimetric Studies: The infrared spectra in the range 400 to 4000 cm^{-1}, were measured on a Bruker IFS 66V FT-IR spectrometer. The samples were ground with dry KBr and pressed into transparent discs. Thermogravimetric analytical data were collected on a Netzsch STA 409C instrument. The samples were heated to 1000 °C at a rate of 10 °C per minute under flowing nitrogen gas.

Supporting Information Available (see footnote on the first page of this article): Color figures showing the polyhedral representation of the unit cells of compounds **1**–**7**.

Acknowledgments

We gratefully acknowledge the financial support (project no. 98/37/29/BRNS) received from the Board of Research in Nuclear Sciences, Government of India. We thank the Sophisticated Analytical Instrument Facility of our institute for collecting the single-crystal X-ray data.

---

[1] R. C. Finn, J. Zubieta, R. C. Haushalter, *Prog. Inorg. Chem.* **2003**, *51*, 421–601.

[2] A. Clearfield, Z. Wang, *J. Chem. Soc., Dalton Trans.* **2002**, 2937–2947.

[3] A. Clearfield, *Prog. Inorg. Chem.* **1998**, *47*, 371–510.

[4] L. A. Vermeulen, *Prog. Inorg. Chem.* **1997**, *44*, 143–166.

[5] A. Clearfield, *Curr. Opin. Solid State Mater. Sci.* **1996**, *1*, 268–278.

[6] M. I. Khan, J. Zubieta, *Prog. Inorg. Chem.* **1995**, *43*, 1–149.

[7] F. Odobel, B. Bujoli, D. Massiot, *Chem. Mater.* **2001**, *13*, 163–173.

[8] a) L. Kullberg, A. Clearfield, *Solvent Extr. Ion Exch.* **1990**, *8*, 187–197; b) C. Y. Ortiz-Avila, C. Bhardwaj, A. Clearfield, *Inorg. Chem.* **1994**, *33*, 2499–2500.

[9] K. Aoki, L. C. Brousseau, T. E. Mallouk, *Sens. Actuators, B* **1993**, *13–14*, 703–704.

[10] a) M. C. C. Costa, R. A. W. Johnstone, D. Whittaker, *J. Mol. Catal. A: Chem.* **1998**, *129*, 79–89; b) K. Segawa, T. Ozawa, *J. Mol. Catal. A: Chem.* **1999**, *141*, 249–255.

[11] a) L. A. Vermeulen, M. E. Thomson, *Nature* **1992**, *358*, 656–658; b) G. Alberti, U. Costantino, M. Casciola, R. Vivani, A. Peraio, *Solid State Ionics* **1991**, *46*, 61–68; c) J. Benavente, F. Carrique, R. Pozas, S. Bruque, L. Moreno, M. Martinez, *Solid State Ionics* **1991**, *46*, 77–82.

[12] a) G. Huan, A. J. Jacobson, V. W. Day, *Angew. Chem. Int. Ed. Engl.* **1991**, *30*, 422–426; b) M. I. Khan, Y.-S. Lee, C. J. O'Connor, R. C. Haushalter, J. Zubieta, *J. Am. Chem. Soc.* **1994**, *116*, 4525–4526; c) S. Drumel, P. Janvier, D. Deniaud, B. Bujoli, *J. Chem. Soc., Chem. Commun.* **1995**, 1051–1052; d) C. B. A. Lima, C. Airoldi, *Int. J. Inorg. Mater.* **2001**, *3*, 907–914.

[13] a) V. Soghomonian, Q. Chen, R. C. Haushalter, J. Zubieta, *Angew. Chem. Int. Ed. Engl.* **1995**, *34*, 223–226; b) G. Alberti, F. Marmottini, S. Murcia-Mascaros, R. Vivani, *Angew. Chem. Int. Ed. Engl.* **1994**, *33*, 1594–1597; c) D. M. Poojary, B. Zhang, P. Bellinghausen, A. Clearfield, *Inorg. Chem.* **1996**, *35*, 4942–4949; d) M. P. Minimol, K. P. Rao, Y. R. Sai, K. Vidyasagar, *Proc. Indian Acad. Sci. (Chem. Sci.).* **2003**, *115*, 419–429; e) K. P. Rao, B. Vidyavathy, M. P. Minimol, K. Vidyasagar, *Inorg. Chem.* **2004**, *43*, 4610–4614.

[14] a) Y.-D. Chang, J. Salta, J. Zubieta, *Angew. Chem. Int. Ed. Engl.* **1994**, *33*, 325–327; b) Y.-D. Chang, J. Zubieta, *Inorg. Chim. Acta* **1996**, *245*, 177–198.

[15] a) K. Maeda, J. Akimato, Y. Kiyozumi, F. Mizukami, *Angew. Chem. Int. Ed. Engl.* **1995**, *34*, 1199–1200; b) W. T. A. Harrison, L. L. Dussack, A. J. Jacobson, *Inorg. Chem.* **1996**, *35*, 1461–1467; c) J. L. Bideau, C. Payen, P. Palvadeau, B. Bujoli, *Inorg. Chem.* **1994**, *33*, 4885–4890.

[16] a) V. Soghomonian, R. C. Haushalter, J. Zubieta, *Chem. Mater.* **1995**, *7*, 1648–1654; b) H. G. Harvey, S. J. Teat, M. P. Attfield, *J. Mater. Chem.* **2000**, *10*, 2632–2633; c) H. G. Harvey, A. C.

Herve, H. C. Hailes, M. P. Attfield, *Chem. Mater.* **2004**, *16*, 3756–3766; d) H. G. Harvey, J. Hu, M. P. Attfield, *Chem. Mater.* **2003**, *15*, 179–188; e) R. N. Devi, P. Wormald, P. A. Cox, P. A. Wright, *Chem. Mater.* **2004**, *16*, 2229–2237; f) M. Bujoli-doeuff, M. Evain, P. Janvier, D. Massiot, A. Clearfield, Z. Gan, B. Bujoli, *Inorg. Chem.* **2001**, *40*, 6694–6698.

[17] a) C. Bellitto, F. Federici, S. A. Ibrahim, *Chem. Mater.* **1998**, *10*, 1076–1082; b) D. M. Poojary, B. Zhang, A. Clearfield, *J. Am. Chem. Soc.* **1997**, *119*, 12550–12559; c) A. Altomare, C. Bellitto, S. A. Ibrahim, M. R. Mahmoud, R. Rizzi, *J. Chem. Soc., Dalton Trans.* **2000**, 3913–3919; d) Q. Gao, N. Guillou, M. Nogues, A. K. Cheetham, G. Férey, *Chem. Mater.* **1999**, *11*, 2937–2947; e) D. I. Arnold, X. Ouyang, A. Clearfield, *Chem. Mater.* **2002**, #*14*#?#*16*#, 2020–2027.

[18] a) C. Serre, G. Ferey, *Inorg. Chem.* **2001**, *40*, 5350–5353; b) F. Serpaggi, G. Ferey, *J. Mater. Chem.* **1998**, *8*, 2749–2755; c) B. A. Adair, G. D. Delgado, J. M. Delgado, A. K. Cheetham, *Solid State Sci.* **2000**, *2*, 119–126.

[19] a) R. Fu, S. Xia, S. Xiang, S. Hu, X. Wu, *J. Solid State Chem.* **2004**, *177*, 4626–4631; b) K. P. Rao, K. Vidyasagar, *Acta Crystallogr., Sect. E* **2005**, *61*, m1794–1796.

[20] K. P. Rao, K. Vidyasagar, *Eur. J. Inorg. Chem.* **2005**, 4936–4943.

[21] K. Yvon, W. Jeitschko, E. Parthe, *J. Appl. Crystallogr.* **1977**, *10*, 73–74.

[22] S. W. Peterson, E. Gebert, A. H. Reis, M. E. Druyan, G. W. Mason, D. F. Peppard, *J. Phys. Chem.* **1977**, *81*, 466–471.

[23] R. M. Silverstein, G. C. Bassler, T. C. Morrill, *Spectrometric Identification of Organic Compounds*, John Wiley & Sons, New York, **1963**, p. 128.

[24] K. J. Frink, R. C. Wang, J. L. Colon, A. Clearfield, *Inorg. Chem.* **1991**, *30*, 1438–1441.

[25] D. Grohol, M. A. Subramanian, D. M. Poojary, A. Clearfield, *Inorg. Chem.* **1996**, *35*, 5264–5271.

[26] G. M. Sheldrick, *SHELXL-97, Program for the Solution of Crystal Structures*, University of Göttingen, Germany, **1985**.

[27] DIAMOND Visual Crystal Structure Information System: W. T. Pennington, *J. Appl. Crystallogr.* **1999**, *32*, 1028–1029.

[28] R.-C. Wang, Y. Zhang, H. Hu, R. R. Frausto, A. Clearfield, *Chem. Mater.* **1992**, *4*, 864–871.

[29] N. Walker, D. Stuart, *Acta Crystallogr., Sect. A* **1983**, *39*, 158–166.

Received: August 17, 2005